Observation of two spin gap energies in the filled skutterudite compound $CeOs_4Sb_{12}$

D. T. Adroja,[1,*] J.-G. Park,[2] E. A. Goremychkin,[1,3] K. A. McEwen,[4] N. Takeda,[5] B. D. Rainford,[6] K. S. Knight,[1] J. W. Taylor,[1] Jeongmi Park,[2] H. C. Walker,[4] R. Osborn,[3] and Peter S. Riseborough[7]

[1]*ISIS Facility, Rutherford Appleton Laboratory, Chilton, Didcot, Oxfordshire, OX11 0QX, United Kingdom*

[2]*BK21 Physics Division, Department of Physics and Institute of Basic Sciences, SungKyunKwan University, Suwon 440-746, Korea and Center for Strongly Correlated Materials Research, Seoul National University, Seoul 151-747, Korea*

[3]*Materials Science Division, Argonne National Laboratory, Argonne, Illinois 60439, USA*

[4]*Department of Physics and Astronomy, University College London, Gower Street, London WC1E 6BT, United Kingdom*

[5]*Faculty of Engineering, Niigata University, Niigata, 950-2181, Japan*

[6]*Department of Physics, Southampton University, Southampton, SO17 1BJ, United Kingdom*

[7]*Department of Physics, Temple University, Barton Hall, 1900N. 13th Street, Philadelphia, Pennsylvania 19122, USA*

(Received 15 June 2006; revised manuscript received 20 October 2006; published 11 January 2007)

The optical conductivity of the Kondo insulator compound $CeOs_4Sb_{12}$ reveals the formation of a 70 meV charge gap below 160 K. It also exhibits a weak shoulderlike structure at 30 meV, below 60 K. We have investigated $CeOs_4Sb_{12}$ by inelastic neutron scattering techniques using incident neutron energies (E_i) of 23 and 200 meV, at 5 and 176 K. Our measurements with E_i=200 meV show magnetic scattering centered near 50–60 meV and low-Q ($\sim$3.8 Å^{-1}) at 5 K, in addition to the continuum of magnetic scattering observed at 176 K. This clearly indicates the opening of a spin gap (or pseudogap) of the order of 50 meV at 5 K in the strongly renormalized band near the Fermi energy. Furthermore, measurements with E_i=23 meV did not reveal any evidence of magnetic excitations below 20 meV, consistent with the scenario of a spin gap in $CeOs_4Sb_{12}$. However, the estimated magnetic scattering deduced from the E_i=200 meV data reveals the presence of broad magnetic scattering between 25 and 80 meV centered near 27 meV, indicating a second energy scale with a gap energy of 27 meV. We interpret the 50 meV energy scale in terms of a direct gap, while the 27 meV energy scale corresponds to an indirect gap across the two hybridized bands. This gap energy of 27 meV is in good agreement with the so-called universal energy scale versus single ion Kondo temperature plot. We present the general features of spin gap systems such as $CeOs_4Sb_{12}$ and $CeRu_4Sb_{12}$, and discuss the role of crystal field excitations regarding the spin gap formation based on a theoretical model.

DOI: 10.1103/PhysRevB.75.014418 PACS number(s): 75.30.Mb, 71.27.+a, 75.20.Hr, 72.15.Qm

INTRODUCTION

Filled skutterudite compounds with the general formula RT_4X_{12} (R=rare-earth, T=transition metal, and X=P, As, and Sb) exhibit various exotic ground state properties, such as metal-insulator transition, unconventional superconductivity, quadrupolar ordering, non-Fermi-liquid behavior, and hybridization gap semiconductor.[1–5] These exotic ground states result from competition between the usual Ruderman-Kittel-Kasuya-Yosida (RKKY) interaction and the on-site screening Kondo interaction.

According to conventional theories of strongly correlated electron systems, the natural consequence of strong hybridization between f electrons and conduction electrons is the opening of a gap in both charge and spin channels.[6–12] Despite their importance, there are few experimental observations of such gaps in real materials. Moreover, the Q dependence of the gap, in particular the spin gap, would provide invaluable information regarding the microscopic mechanism of the gap formation. Recently we have investigated the formation of the spin gap and its relation to the charge gap, in Ce, Yb, and U compounds using inelastic neutron scattering techniques.[13–16] So far, we have successfully demonstrated that such a hybridization gap indeed occurs at low temperatures in the magnetic excitation spectrum of $CeRu_4Sb_{12}$ with the spin gap energy of Δ_{spin}=30 meV compared with the charge gap (from optical studies) of Δ_{char}=47 meV.[5,13] On the other hand, a spin gap of 150 meV is found for CeRhAs, somewhat higher than the charge gap of 100 meV measured from the x-ray photoemission spectroscopy (XPS) measurements.[16] However, despite the efforts by ourselves and other authors, it is still worth investigating spin and charge gaps in many other strongly correlated electron systems in order to understand better their microscopic mechanism and compare the experimental results with theoretical predictions.

Transport property measurements indicate that the skutterudite compound $CeOs_4Sb_{12}$ exhibits Kondo insulating behavior with a very small transport gap of 10 K.[17,18] The resistivity of $CeOs_4Sb_{12}$ is metallic at room temperature, but increases strongly, with decreasing temperature, below 50 K. The two reported values of the specific heat coefficient, $\gamma \sim 90$ and 180 mJ mole^{-1} K^{-2} (Refs. 17, 19, and 20) and enhanced Pauli-susceptibility indicate a strongly correlated electron behavior of $CeOs_4Sb_{12}$.[17] The susceptibility exhibits a broad maximum near 100 K, which can be explained using either a crystalline electric field (CEF) model with a CEF splitting of $\sim$28 meV for the Ce^{3+} ion[17] or a valence fluctuation model. Recent optical conductivity studies[21] show a strongly temperature dependent response with a pronounced peak at 70 meV below 160 K, and a weak shoulder at 30 meV below 60 K. Thus $CeOs_4Sb_{12}$ is a system with charge gaps in the strongly hybridized band near the Fermi energy, E_F. The peak at 70 meV was interpreted in terms of an optical excitation across the direct gap with a momentum

conserving ($\partial Q=0$) dipole allowed transition between the two hybridized bands. On the other hand, the origin of the weak shoulder at 30 meV was tentatively attributed to an optically forbidden transition ($\partial Q \neq 0$), which might be allowed with a weak intensity in the presence of defects or an impurity.[21]

The key question regarding the charge gap feature found in $CeOs_4Sb_{12}$ is whether it is somehow connected to spin degrees of freedom so as to produce a corresponding spin gap in the magnetic excitation spectrum, which is then observable by inelastic neutron scattering. If such a spin gap indeed exists, then it is important to determine whether it is Q dependent (indicating intersite coupling) or Q independent (i.e., a single ion feature). An experimentally determined ratio between the spin gap and the charge gap is also important for a theoretical point of view. Furthermore, we would like to understand the origin of 30 meV peak in the optical study and the nature of the $4f$ electrons in $CeOs_4Sb_{12}$. This information would be of particular significance in understanding the origin of the gap formation in $CeOs_4Sb_{12}$. It should be emphasised that although the optical studies were successful in finding the charge gap they cannot offer any further information about the Q dependence of the gap, due to the limitations of this technique: any indirect optical transitions (i.e., $\partial Q \neq 0$) are forbidden by the momentum conservation rule within the first order optical processes.[22] However, we note that nondipolar transitions with $\partial Q \neq 0$ are possible in the second order optical process through which a two-phonon process occurs.[23]

In order to answer these questions, we have carried out inelastic neutron scattering measurements on $CeOs_4Sb_{12}$ and the isostructural nonmagnetic reference compound $LaOs_4Sb_{12}$. Our results show clear evidence of a spin gap or pseudogap of 50 meV as well as a second energy gap of 27 meV in $CeOs_4Sb_{12}$ at 5 K. We interpret these two gaps in terms of direct and indirect transitions, respectively.

EXPERIMENTAL

Our samples of polycrystalline $CeOs_4Sb_{12}$ and $LaOs_4Sb_{12}$ were synthesized at Niigata University, Japan following the synthesis recipe given in Ref. 24. Ce, La, and Os with 99.9% and Sb with 99.999% purity were used as the starting materials. Our subsequent x-ray powder diffraction study showed that both samples formed in the body-centered cubic structure, with almost no trace of secondary phases at 300 K. We carried out a further study of the crystal structure of $CeOs_4Sb_{12}$ at 300 K using the high resolution neutron powder diffractometer HRPD at ISIS, UK. The magnetic susceptibility of $CeOs_4Sb_{12}$ was measured using a commercial SQUID magnetometer (Quantum Design MPMS-5XL, USA). Inelastic neutron scattering measurements on $CeOs_4Sb_{12}$ and on the nonmagnetic reference compound $LaOs_4Sb_{12}$ were carried out using the time-of-flight chopper spectrometer HET at ISIS, with incident neutron energies (E_i) of 23 and 200 meV at 5 and 176 K. The observed scattering intensity was converted into absolute units of mb/sr/meV/f.u. by normalizing the measured scattering intensity to that from a standard Vanadium sample. We also made corrections to the data for sample absorption and attenuation using a flat-plate geometry option available in the ISIS data reduction program.

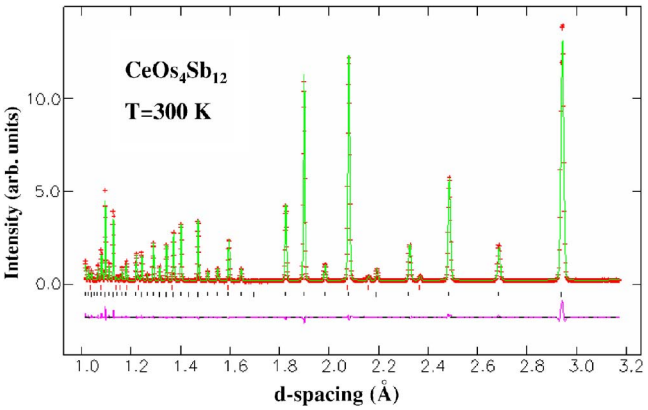

FIG. 1. (Color online) Powder neutron diffraction pattern from $CeOs_4Sb_{12}$ taken at 300 K using the HRPD diffractometer at ISIS. Symbols are for the data points while the line underneath them is for the refinement results. Two rows of vertical bars correspond to the phases of $CeOs_4Sb_{12}$ (bottom), pure Os metal (top). The line at the bottom is for the difference curve.

III. RESULTS AND DISCUSSION

A. Neutron diffraction

Rietveld analysis of our neutron diffraction data at 300 K using the GSAS program confirmed that $CeOs_4Sb_{12}$ crystallizes in the Im-3 space group (No 204) and that the sample was of high quality. We found weak impurity peaks, corresponding to about 1.8% in volume, of pure Os metal, which crystallizes in the hexagonal structure with lattice parameters $a=2.73412(1)$ Å and $c=4.3193(1)$ Å (see Fig. 1). For the structure refinement of $CeOs_4Sb_{12}$, we have assigned Ce on $2a$ (0 0 0), Os on $8c$ (1/4,1/4,1/4), and Sb on 24 g $(0,y,z)$ crystallographic sites. The estimated value of the cubic lattice parameter $a=9.303\,59(4)$ Å, compared with 9.299 Å at 5 K,[25] and the atomic position parameters of Sb atoms are $x_{Sb}=0$, $y_{Sb}=0.156\,278(8)$, and $z_{Sb}=0.340\,55(8)$. The occupancy and isotropic thermal factors were also refined in our analysis. The values of the occupancy factors are 1.01(1) for Os and 1.04(1) for Sb (the occupancy of Ce was kept fixed at 1.000 during the Rietveld refinement), which corresponds to full occupancy of all the atoms. The isotropic thermal factors (in $Å^2$) are 0.0420(16) for Ce, 0.0097(3) for Os, and 0.0062(6) for Sb. It is to be noted that the larger value of the isotropic temperature factor observed for the Ce atom is consistent with the rattling motion expected for the Ce atoms in this structure. Our observation is also consistent with the extended x-ray-absorption fine structure (EXAFS) studies on various skutterudites.[25] The low value of the Einstein temperature $\theta_E=71$ K obtained for the Ce-Sb pairs in $CeOs_4Sb_{12}$ strongly supports the concept of a "rattling" local mode behavior for the Ce ions. Furthermore, the EXAFS analysis also indicates that this rattling frequency is much smaller in the antimonide skutterudites than in the phosphide ones.[25]

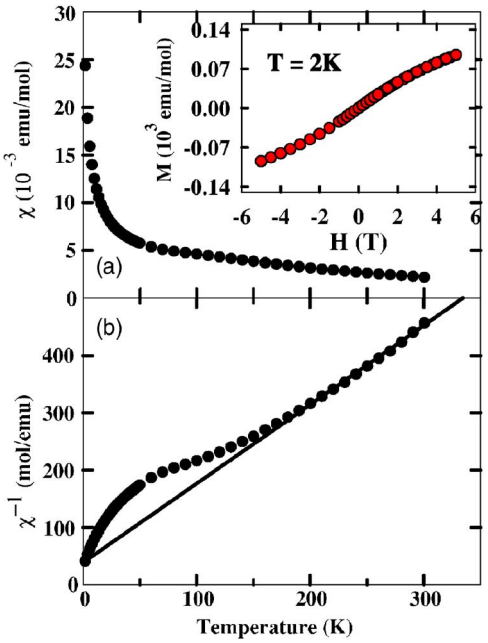

FIG. 2. (Color online) Temperature dependence of (a) magnetic susceptibility and (b) inverse magnetic susceptibility of $CeOs_4Sb_{12}$. The solid line (in b) represents the Curie-Weiss fit. The inset in (a) shows the magnetization data at 2 K.

This result indicates that the larger the void within which the Ce atom is located, the lower its rattling frequency. The bond distances obtained at 300 K are Ce-Sb=3.4860(9) Å, Ce-Os=4.0285(1) Å compared with those reported at 5 K of 3.47 and 4.00 Å, respectively.[25] Therefore the change in the Ce-Sb distance is barely 0.46% compared with 0.71% for Ce-Os. These smaller changes in the atomic distances may suggest that the lattice degrees of freedom are not playing an important role in the gap formation in $CeOs_4Sb_{12}$.

B. Magnetic susceptibility

Figures 2(a) and 2(b) shows the temperature dependence of the magnetic susceptibility and inverse susceptibility of $CeOs_4Sb_{12}$ measured in an applied field of 0.1 T. The susceptibility is weakly temperature dependent between 50 and 300 K, displaying a broad hump centered near 100 K. The inverse susceptibility exhibits Curie-Weiss behavior between 200 and 300 K with an effective paramagnetic moment μ_{eff} =2.41 μ_B/Ce atom and a Curie-Weiss temperature θ_{CW}= −28 K. Our susceptibility results are in agreement with those previously published.[17] However, there is a certain difference in the values of μ_{eff} and θ_{CW}, which may be due to the different temperature range used for the estimate of the parameters, or to a difference in the impurity contribution. For example, the observed low-temperature rise in the susceptibility was attributed in Ref. 17 to an impurity contribution, after estimating the Pauli susceptibility from the high field magnetization measurements. Bauer *et al.*[17] analyzed their susceptibility data using a cubic CEF model, which gave a crystal field splitting of ~31 meV between the ground state doublet Γ_7 and the excited quartet Γ_8. However, the previous

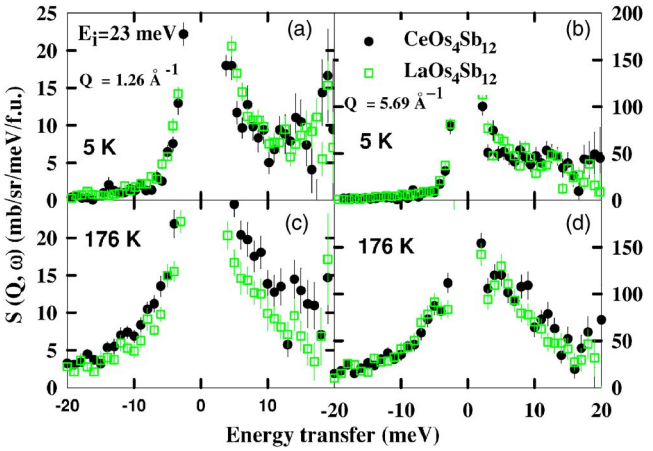

FIG. 3. (Color online) (a–d) The observed scattering from $CeOs_4Sb_{12}$ and $LaOs_4Sb_{12}$ measured with an incident neutron energy E_i=23 meV at low Q and high Q at 5 and 176 K.

neutron scattering measurements by Yang *et al.*[26] and our present results, discussed below, do not show any clear sign of a well-defined crystal field excitation: we have observed only a very broad inelastic response at 27 meV. The inset in Fig. 2(a) shows our magnetization measurements at 2 K: the almost linear behavior observed here is that expected for the paramagnetic ground state of $CeOs_4Sb_{12}$.

C. Inelastic neutron scattering

Figures 3(a)–3(d) shows the observed scattering from $CeOs_4Sb_{12}$ and $LaOs_4Sb_{12}$ measured with E_i=23 meV at low Q (1.26 Å^{-1}) and high Q (5.69 Å^{-1}) at 5 and 176 K. As one can see in Fig. 3(a), there is no clear evidence of quasielastic magnetic scattering below 20 meV in $CeOs_4Sb_{12}$ at 5 K. On the other hand, it is noticeable that at 176 K there is significantly stronger scattering at low Q for $CeOs_4Sb_{12}$ than for $LaOs_4Sb_{12}$ [see Fig. 3(c)]. This indicates the presence of quasielastic magnetic scattering in $CeOs_4Sb_{12}$ at high temperature. This was further confirmed by our estimate of the magnetic scattering from $CeOs_4Sb_{12}$ using the following method:[13]

$$S(Q,\omega)_{\text{Mag}} = S(Q,\omega)_{\text{CeOs4Sb12}} - S(Q,\omega)_{\text{LaOs4Sb12}} \times \alpha,$$

where the scaling factor α is the ratio of the total scattering cross section of $LaOs_4Sb_{12}$ to $CeOs_4Sb_{12}$. This ratio is estimated to be ~1.0 after taking into account the relatively small sample masses (~8 g). Figure 4 shows the estimated magnetic scattering from $CeOs_4Sb_{12}$ at 5 and 176 K with E_i=23 meV. Again, there is no magnetic scattering at 5 K while at 176 K we can see a clear presence of quasielastic scattering. These results demonstrate that there is no clear magnetic scattering up to 20 meV at 5 K, i.e., a spin gap, which upon heating becomes a quasielastic response at 176 K. This observation seems to be in agreement with the temperature dependent response observed in the optical study.[21] Using the Kramers-Krönig relation (discussed below in more detail), we estimate the Curie contribution of the susceptibility at 176 K as $\sim 2.7(3) \times 10^{-3}$ emu/mol based on the measured quasielastic response.

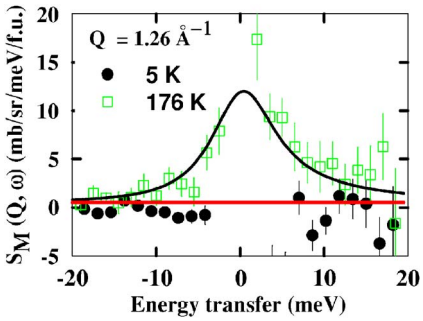

FIG. 4. (Color online) Magnetic scattering from $CeOs_4Sb_{12}$ at 5 and 176 K, measured with E_i=23 meV. The solid line represents the fit to a Lorentzian function.

In order to cover a larger range of energy and wave vector (Q) transfer, we carried out inelastic neutron scattering measurements using a higher incident neutron energy of E_i =200 meV with the aim of determining the excitation spectrum corresponding to the 70 meV charge gap observed in the optical study.[21] Figures 5(a)–5(d) show the observed scattering intensity from $CeOs_4Sb_{12}$ and $LaOs_4Sb_{12}$ at 5 and 176 K at low Q (3.8 Å^{-1}) and high Q (15.1 Å^{-1}). There is noticeably a higher scattering intensity around energy transfers of 50–60 meV at low Q in $CeOs_4Sb_{12}$ at 5 K than at 176 K. Although the intensity change is relatively small, nevertheless it is a genuine response from the sample, as one does not expect a large change in the population factor for excitations near 60 meV (692 K) by increasing the temperature from 5 to 176 K. This has been further confirmed by the observation that there are no such changes in the $LaOs_4Sb_{12}$ data [Figs. 5(c) and 5(d)] for both low and high Q as well as the high-angle data of $CeOs_4Sb_{12}$ [Fig. 5(b)]. This change in the intensity becomes clearer when the data from the 4 and 2.5 m detector banks of the HET spectrometer (at scattering angles of 4.9° and 19°, respectively) are plotted separately [see insets of Figs. 5(b) and 5(d)]. We therefore interpret the

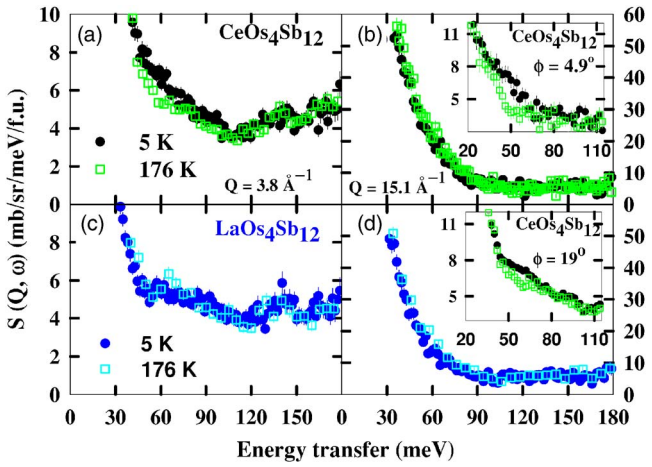

FIG. 5. (Color online) (a–d) The observed scattering from $CeOs_4Sb_{12}$ (a,b) and $LaOs_4Sb_{12}$ (c,d) measured with an incident neutron energy E_i=200 meV at low Q and high Q at 5 and 176 K. The insets show the low angle data from the 4 m bank (top) at 2Θ=4.9° and the 2.5 m bank (bottom) at 2Θ=19°.

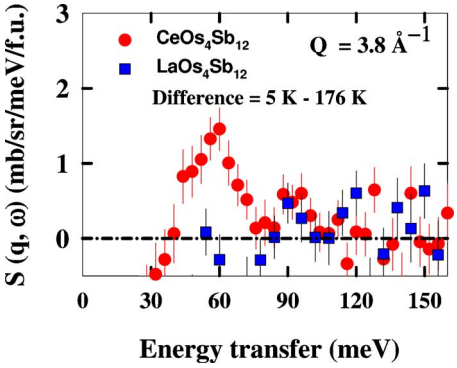

FIG. 6. (Color online) The difference between two scattering data sets taken at 5 and 176 K from $CeOs_4Sb_{12}$ and $LaOs_4Sb_{12}$ measured with an incident neutron energy E_i=200 meV at low Q.

observed change in the intensity near 50–60 meV as due to a magnetic excitation from the lower hybridized 4f band to the upper hybridized 4f band near the Fermi level [see the inset Fig. 7(b)]. In order to confirm the magnetic nature and Q dependence of the 50–60 meV peak in $CeOs_4Sb_{12}$, we have estimated the magnetic scattering using the following two methods: (i) direct subtraction of the two data sets, i.e., $S_{5\ K}-S_{176\ K}$, and (ii) correcting the 176 K data for the population factor before the subtraction, i.e., $S_{5\ K}-S_{176\ K}\times$ Bose factor (5 K)/Bose factor (176 K). A similar analysis was also carried out for the $LaOs_4Sb_{12}$ data. The difference spectra obtained from both methods produced a peak in the inelastic response at ~60 meV for $CeOs_4Sb_{12}$, but not for $LaOs_4Sb_{12}$ (see Fig. 6, method i). The peak position was found to have a clear Q dependence: ~50 meV at Q=1.5 Å^{-1} and 59 meV at Q=3.3 Å^{-1} (see the insets of Fig. 5). Moreover, the integrated intensity from 40 to 80 meV decreases with increasing Q and follows as expected the Ce^{3+} magnetic form factor squared, $F^2(Q)$, confirming the magnetic nature of the scattering.

To check further the presence of a lower energy excitation as observed near 30 meV in the optical study, we have estimated the magnetic scattering in $CeOs_4Sb_{12}$ by subtracting off the phonon contribution using the $LaOs_4Sb_{12}$ data. The estimated magnetic scattering of $CeOs_4Sb_{12}$ at 5 K is shown in Fig. 7(a). The inset shows clearly that the magnetic scattering is greater at 5 K than at 176 K. The vertical arrows indicate the position of the charge gaps observed in the optical study.[21] At 5 K, the magnetic scattering has a peak around 27 meV and extends as high as 80 meV. Furthermore, the estimated magnetic scattering at 176 K shows similar behavior, but with a much reduced intensity between 25 and 80 meV [inset Fig. 7(a)]. Again the Q dependence of the energy integrated intensity between 30 and 75 meV follows, as expected, the square of the Ce^{3+} magnetic form factor [see Fig. 7(b)]. It is also interesting to calculate the magnetic susceptibility from the observed inelastic magnetic response and compare this value with that of the bulk susceptibility. Using the sum rule for the uniform bulk susceptibility (the so-called Kramers-Krönig relation), $\int \chi''(\omega)/\omega\, d\omega = \chi'(0)$, and taking a numerical integration of the data, we have estimated $\chi'(0)=5.9(1)\times 10^{-3}$ emu/mol at 5 K. This value of the susceptibility is comparable to the value esti-

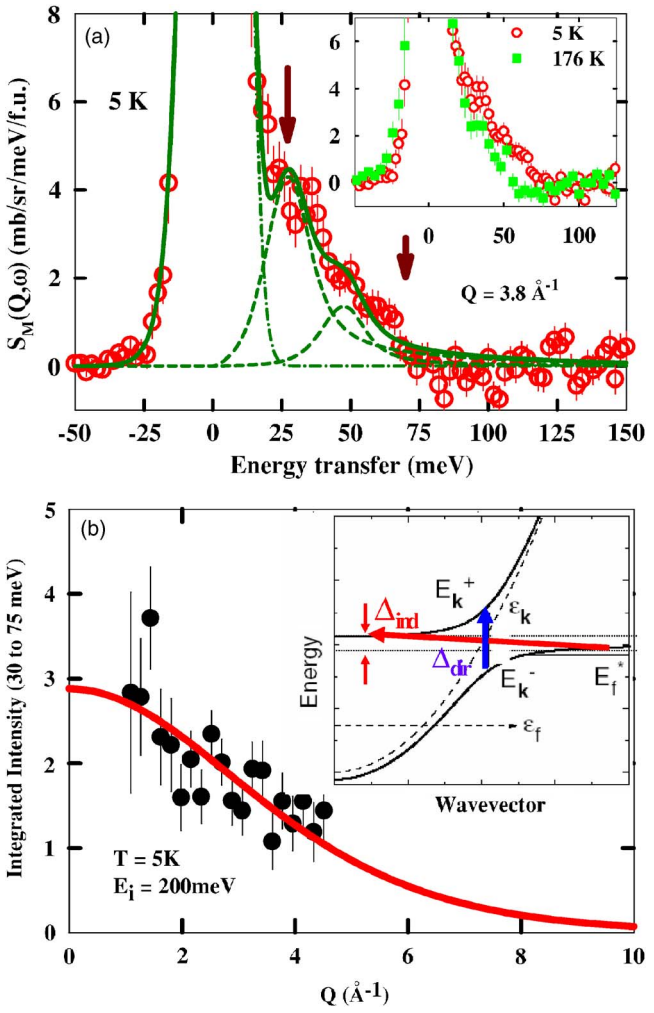

FIG. 7. (Color online) (a) The estimated magnetic scattering of $CeOs_4Sb_{12}$ at 5 K after subtracting the scattering from $LaOs_4Sb_{12}$ (see text). The solid and dash lines represent the fit using two Lorentzian functions (see text). The inset shows the magnetic scattering at 5 K and 176 K for comparison. (b) It shows the Q dependence of the total intensity integrated between 30 and 75 meV at 5 K (symbols) and the square of the Ce^{3+} magnetic form factor (solid line, scaled to 2.88 at $Q=0$) (Ref. 39). The inset in (b) shows a schematic picture of the hybridized bands (solid lines) and possible interband transitions (direct and indirect) shown by the arrows with energy transfer (ΔE) and momentum transfer (∂Q) from Ref. 6. The dotted lines represent the unhybridized $4f$ band (ε_f) and conduction band (ε_k).

mated from the high field magnetization measurements $\sim 9(1)\times 10^{-3}$ emu/mol, but smaller than the bulk susceptibility $\sim 20(1)\times 10^{-3}$ emu/mol.[17] It is to be noted that our estimate of the susceptibility using the inelastic neutron data contains the Van-Vleck contribution but not any Curie-like contribution, which may arise from a quasielastic response, if present. Unfortunately, however, our present experimental resolution was not sufficient to detect any narrow quasielastic line. The estimated value of the Van-Vleck contribution to the susceptibility from the 200 meV data taken at 176 K is $1.7(7)\times 10^{-3}$ emu/mol. Thus the total contribution to the susceptibility at 176 K (from both 23 and 200 meV data) is $4.4(8)\times 10^{-3}$ emu/mol, which is in better agreement with the measured bulk susceptibility.

We have analyzed our magnetic scattering data at 5 K taken with $E_i=200$ meV using a single Lorentzian function convoluted with the instrument resolution function [see Fig. 7(a)]. However, this approach does not give a good fit to the data between 40 and 80 meV. Thus we have used *two* Lorentzian functions, which improve the fit in this energy range [see Fig. 7(a), the solid line represents the fit and the dash lines represent the components of the fit], and yields peaks centered at 27(2) meV and 48(2) meV with linewidth 5.2 meV for both. The value of $\chi'(0)$ estimated from the total intensity of these peaks is $4.0(5)\times 10^{-3}$ emu/mol, in agreement with that estimated by the previous numerical integration method. This analysis seems to support our claim that there exist two energy gaps in the inelastic response of $CeOs_4Sb_{12}$, which is in agreement with the optical study.[21]

The observed magnetic response in $CeOs_4Sb_{12}$ raises several interesting questions. The first question concerns the nature of the gaps around 27 and 48 meV. Possible explanations could be in terms of a crystal field excitation (Γ_7 to Γ_8) as interpreted in the magnetic susceptibility in Ref. 17 or a spin gap formation in the strongly hybridized band near E_F corresponding to the charge gap of a similar magnitude as observed in the optical study.[21] However, the explanation based on the crystal field excitation has obvious limitations here. For example, one cannot have two CEF excitations for a Ce^{3+} ion in cubic symmetry. Furthermore, we note that the isostructural compounds $PrOs_4Sb_{12}$ and $PrRu_4Sb_{12}$ exhibit very sharp CEF excitations.[27,28] Using the CEF parameters obtained for $PrOs_4Sb_{12}$ and scaling them with a simple point change model, we estimate a CEF splitting of 7.4 meV for $CeOs_4Sb_{12}$ with Γ_8 as the ground state. Thus we consider that the observed magnetic response in $CeOs_4Sb_{12}$ cannot be due to a pure crystal field-type excitation, but is most likely to be dominated by the presence of strong hybridization effects. Theoretical models predict that the strong hybridization present in Kondo lattice systems should open an energy gap near E_F.[6] Hence, we attribute the observed response to a spin gap formation near E_F. As we have observed spin gap signatures at $\sim$27 meV and at $\sim$50 meV, we propose naturally that they should correspond to the charge gaps of 30 and 70 meV as observed in the optical study. Therefore, our data and interpretation show that the observed ratio of the spin and charge gaps is 0.7–0.9 (using the peak positions from our fit) for $CeOs_4Sb_{12}$. This is in accord with the theoretical prediction of 0.7–0.9 for the Anderson Lattice Model (ALM) with infinite dimension: for the one-dimensional (1D) ALM the ratio is predicted to be around 0.3–0.4.[9,10,30,31]

We now address our second question: whether there is any common feature between the spin gap formation experimentally observed in both $CeOs_4Sb_{12}$ and $CeRu_4Sb_{12}$. It is conceivable that the observed response near 27 meV in $CeOs_4Sb_{12}$ has something in common with that observed in $CeRu_4Sb_{12}$ and many intermediate valence Ce compounds.[6,13–16,29] However, the strong temperature dependence of the excitation observed in $CeOs_4Sb_{12}$ near 50–60 meV, in addition to the broad magnetic response, is a unique feature, not observed in other Ce based compounds. There is also an interesting and perhaps important difference

to be noticed in $CeRu_4Sb_{12}$, $Ce_3Pt_3Bi_4$ and other spin gap systems in that the temperature dependent susceptibility exhibits a clear and pronounced broad maximum for these systems, which is not the case in $CeOs_4Sb_{12}$ (the maximum is very weak). As we noted before, the observed broad hump in the susceptibility of $CeOs_4Sb_{12}$ was explained in terms of a CEF model.[17] This then opens up a very interesting possibility that crystal field effects play some role in the spin gap formation and hence the bulk properties of $CeOs_4Sb_{12}$. The importance of a certain CEF ground state for the opening of an anisotropic spin gap has been discussed theoretically for CeNiSn.[11,12]

Our third question concerns the origin of the two energy scales, 27 and 50–60 meV, seen in our inelastic neutron scattering results. This experimental observation is particularly unusual. However, we note that two energy scales have been observed in recent studies of polycrystalline $YbAl_3$ and single crystal studies of $YbAl_3$ and YbB_{12}.[32–35] Following the discussions given in these publications, we can interpret the low energy excitation seen at 27 meV as an indirect excitation, with $\partial Q \neq 0$, across the hybridized bands, while the higher energy excitation at 50–60 meV may originate from a direct excitation across the hybridized bands with $\partial Q = 0$ [see the inset in Fig. 7(b)]. The intensity of inelastic transitions in interband scattering (i.e., indirect and direct transitions) is proportional to the product of the density of states in the initial and final states.[32] Theoretical calculations show that the top of the lower band and bottom of the upper band are strongly dominated by $4f$ density of states and the remaining part of the bands are dominated by conduction electrons, hence low density of states.[6] Therefore, the intensity of the low energy peak (i.e., the indirect excitation) is expected to be stronger than that of the high energy peak (i.e., the direct excitation). In this scenario, the most intense peak occurs at the threshold value of energy transfer for the indirect transitions from the zone boundary of the lower band to the zone center of the upper band.

Recently a theoretical model was proposed for the pseudogap formation in Ce, Sm, Eu, and Yb based compounds by Hanzawa *et al.*,[36] who discussed the various limits of CEF and its roles in the gap formation. Their model considered a variety of energy gap features depending on the strength and symmetry of the CEF. The three cases they discussed are: (i) No CEF effect—in this case a fully isotropic gap opens at the Fermi level, (ii) Large CEF effect—if the CEF splitting is huge then an anisotropic full or pseudogap opens, and (iii) Intermediate CEF effect—when $\Delta_{CEF} \sim \Delta_{gap}$, then rather complicated but interesting features appear in the gap formation.[36] As shown for the $J=5/2$ Sm^{3+} case with a cubic crystal field, a full gap opens for the case of the Γ_8 ground state, while a small but finite density of states remains in the pseudogap region for the Γ_7 ground state. Although Hanzawa *et al.* did not discuss the case of Ce^{3+}, it is not unrealistic that as Ce^{3+} also has $J=5/2$ the observed temperature dependence of the susceptibility and the high γ value of $CeOs_4Sb_{12}$ may well be explained qualitatively with the Γ_7 ground state model and finite density of states at E_F. This finite density of states can then give a high value of γ and Curie-type rise in the susceptibility.

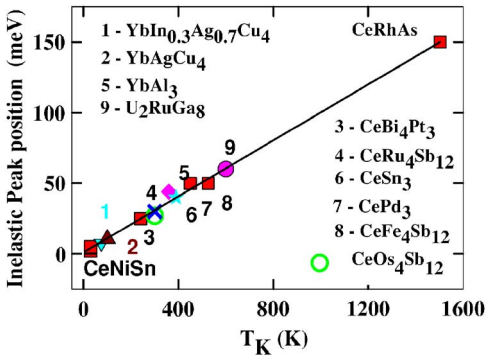

FIG. 8. (Color online) The estimated spin gap (i.e., peak position of inelastic response) versus Kondo temperature, T_K for several heavy fermion systems: T_K is taken as three times the temperature at which the dc susceptibility exhibits a maximum [$T_K = 3^* T(\chi_{maxi})$, see the text]. The solid line represents a linear behavior. The data of $CeFe_4Sb_{12}$ and U_2RuGa_8 are taken from Refs. 40 and 41.

In this connection, it is very interesting to note that a recent study of the nuclear-spin relaxation rate $1/T_1$, measured using Sb-NQR, of $CeOs_4Sb_{12}$ showed the presence of a gap $\Delta_{NMR}=27.6$ meV with a finite residual density of states (DOS), $N/N_{res}=0.3$ at the Fermi level.[37] The value of the gap estimated from the nuclear quadrupole resonance (NQR) study is remarkably similar to the spin gap of 27 meV (low energy gap) found in our neutron scattering studies.

According to a single ion impurity Anderson model,[38] the Kondo temperature T_K is related to the temperature T_{max} at which the bulk susceptibility exhibits a maximum, i.e., $T_K = 3T_{max}$. In order to compare the magnitude of the spin gaps observed in $CeOs_4Sb_{12}$ with that of the single ion Kondo temperature, we have plotted the inelastic peak position versus T_K (i.e., three times T_{max}) in Fig. 8, of $CeOs_4Sb_{12}$ along with many Ce and Yb systems. It is clear from Fig. 8 that the spin gap increases linearly with T_K ($\sim 3T_{max}$) and exhibits a universal behavior for Ce and Yb systems. Further, the gap of 27 meV (obtained from the peak position) of $CeOs_4Sb_{12}$ lies on the universal line, whereas the 50–60 meV gap (not shown in Fig. 8) exhibits a considerable deviation. This indicates that the 27 meV indirect gap in $CeOs_4Sb_{12}$ has a single-ion nature. It is to be noted that our present study using a polycrystalline sample cannot discuss the exact nature of the 50–60 meV excitation. For this, we would need to study single crystal $CeOs_4Sb_{12}$: unfortunately, sufficiently large crystals are not yet available.

CONCLUSIONS

In conclusion, we have carried out inelastic neutron scattering measurements on $CeOs_4Sb_{12}$ and the nonmagnetic reference $LaOs_4Sb_{12}$ to study the spin gap formation in the former. Our inelastic neutron scattering study with $E_i = 23$ meV does not reveal any magnetic scattering below 20 meV at 5 K, but shows the presence of quasielastic scattering at 176 K. Furthermore, our measurements with $E_i = 200$ meV clearly show the presence of two energy scales, 27 and 50–60 meV, which we attribute to an indirect exci-

tation and a direct excitation across the hybridized bands near the Fermi energy in agreement with the previous optical study. The spin gap of 27 meV seems to follow a universal scaling behavior with the Kondo energy estimated from the bulk susceptibility, and hence the single ion Kondo interaction seems to be responsible for the spin gap formation. On the other hand, the 50–60 meV excitation shows a strong temperature dependence as well as a weak Q dependence, suggesting the effect of lattice coherence is also playing an important role in the spin gap formation in $CeOs_4Sb_{12}$. We hope that our present study will stimulate new theoretical investigations that might lead to a complete understanding of the two observed energy scales in $CeOs_4Sb_{12}$ as well as in $YbAl_3$ and YbB_{12}.

ACKNOWLEDGMENTS

We are grateful to Amir Murani for stimulating discussions and the ISIS Facility for providing the beam time and financial support. One of us (J.G.P.) acknowledges financial support by the BAERI program, the CNRF project, and the Korea Research Foundation (Grant No. 2005-C00153). E.A.G and R.O. were supported by the US Department of Energy, Office of Science, under Contract No. W-31-109-ENG-38.

*Corresponding author. Electronic address: d.t.adroja@rl.ac.uk

[1] C. Sekine, T. Uchiumi, I. Shirotani, and T. Yagi, Phys. Rev. Lett. **79**, 3218 (1997).

[2] E. D. Bauer, N. A. Frederick, P.-C. Ho, V. S. Zapf, and M. B. Maple, Phys. Rev. B **65**, 100506(R) (2002); N. R. Dilley, E. J. Freeman, E. D. Bauer, and M. B. Maple, Phys. Rev. B **58**, 6287 (1998).

[3] H. Sato, Y. Abe, H. Okada, T. D. Matsuda, K. Abe, H. Sugawara, and Y. Aoki, Phys. Rev. B **62**, 15125 (2000).

[4] N. Takeda, and M. Ishikawa, J. Phys. Soc. Jpn. **69**, 868 (2000); N. Takeda, Physica B **281**, 388 (2000).

[5] S. V. Dordevic, D. N. Basov, N. R. Dilley, E. D. Bauer, and M. B. Maple, Phys. Rev. Lett. **86**, 684 (2001).

[6] See for example, P. S. Riseborough, Adv. Phys. **49**, 257 (2000); Phys. Rev. B **45**, 13984 (1992).

[7] A. J. Millis and P. A. Lee, Phys. Rev. B **35**, 3394 (1987); A. J. Millis, M. Lavagna, and P. A. Lee, *ibid.* **36**, 864 (1987).

[8] B. H. Brandow, Phys. Rev. B **37**, 250 (1988).

[9] A. Georges, G. Kotliar, W. Krauth, and M. J. Rozenberg, Rev. Mod. Phys. **68**, 13 (1996).

[10] M. J. Rozenberg, G. Kotliar, and H. Kajueter, Phys. Rev. B **54**, 8452 (1996).

[11] J. Moreno and P. Coleman, Phys. Rev. Lett. **84**, 342 (2001); G. Aeppli and Z. Fisk, Comments Condens. Matter Phys. **16**, 155 (1992).

[12] H. Ikeda and K. Miyake, J. Phys. Soc. Jpn. **65**, 1769 (1996).

[13] D. T. Adroja, J.-G. Park, K. A. McEwen, N. Takeda, M. Ishikawa, and J.-Y. So, Phys. Rev. B **68**, 094425 (2003).

[14] D. T. Adroja, J.-G. Park, K. A. McEwen, N. Takeda, and M. Ishikawa, J. Magn. Magn. Mater. **272**, E21 (2004).

[15] K. A. McEwen, D. T. Adroja, J.-G. Park, and A. D. Hillier (unpublished).

[16] D. T. Adroja, J.-G. Park, K. A. McEwen, K. Shigetoh, T. Sasakawa, T. Takabatake, and J. Y. So, Physica B **378**, 788 (2006).

[17] E. D. Bauer, A. Slebarski, E. J. Freeman, C. Sirvent, and M. B. Maple, J. Phys.: Condens. Matter **13**, 4495 (2001); M. Hedo, Y. Uwatoko, H. Sugawara, and H. Sato, Physica B **329**, 456 (2003).

[18] H. Sugawara, S. Osaki, M. Kobayashi, T. Namiki, S. R. Saha, Y. Aoki, and H. Sato, Phys. Rev. B **71**, 125127 (2005).

[19] T. Namiki, Y. Aoki, H. Sugawara, and H. Sato, Acta Phys. Pol. B **34**, 1161 (2003).

[20] C. R. Rotundu and B. Andraka, Phys. Rev. B **73**, 144429 (2006).

[21] M. Matsunami, H. Okamura, T. Namba, H. Sugawara, and H. Sato, J. Phys. Soc. Jpn. **72**, 2722 (2003).

[22] M. Dressel and G. Gruner, *Electrodynamics of Solids* (Cambridge University Press, Cambridge, 2002).

[23] P. Y. Yu and M. Cardona, *Fundamentals of Semiconductors* (Springer, Berlin, 2001) 3rd edition, Chap. 6.2.; H. Okamura, T. Michizawa, T. Nanba, S. Kimura, F. Iga, and T. Takabatake, J. Phys. Soc. Jpn. **74**, 1954 (2005).

[24] N. Takeda and M. Ishikawa, J. Phys.: Condens. Matter **13**, 5971 (2001).

[25] D. Cao, F. Bridges, P. Chesler, S. Bushart, E. D. Bauer, and M. B. Maple, Phys. Rev. B **70**, 094109 (2004).

[26] C. Yang, M. Kohgi, K. Iwasa, H. Sugawara, and H. Sato, J. Phys. Soc. Jpn. **74**, 2862 (2005).

[27] E. A. Goremychkin, R. Osborn, E. D. Bauer, M. B. Maple, N. A. Frederick, W. M. Yuhasz, F. M. Woodward, and J. W. Lynn, Phys. Rev. Lett. **93**, 157003 (2004).

[28] A. Severing, J. D. Thompson, P. C. Canfield, Z. Fisk, and P. Riseborough, Phys. Rev. B **44**, 6832 (1991).

[29] D. T. Adroja, J.-G. Park, E. A. Goremychkin, N. Takeda, M. Ishikawa, K. A. McEwen, R. Osborn, A. D. Hillier, and B. D. Rainford, Physica B **359**, 983 (2005).

[30] C. Gröber, and R. Eder, Phys. Rev. B **57**, R12659 (1998).

[31] B. Bucher, Z. Schlesinger, P. C. Canfield, and Z. Fisk, Phys. Rev. Lett. **72**, 522 (1994).

[32] A. D. Christianson, V. R. Fanelli, J. M. Lawrence, E. A. Goremychkin, R. Osborn, E. D. Bauer, J. L. Sarrao, J. D. Thompson, C. D. Frost, and J. L. Zarestky, Phys. Rev. Lett. **96**, 117206 (2006).

[33] J.-M. Mignot, P. A. Alekseev, K. S. Nemkovski, L.-P. Regnault, F. Iga, and T. Takabatake, Phys. Rev. Lett. **94**, 247204 (2005).

[34] P. A. Alekseev, J.-M. Mignot, K. S. Nemkovski, E. V. Nefeodova, N. Yu. Shitsevalova, Yu. B. Paderno, R. I. Bewley, R. S. Eccleston, E. S. Clementyev, V. N. Lazukov, I. P. Sadikov, and N. N. Tiden, J. Phys.: Condens. Matter **16**, 2631 (2004).

[35] A. P. Murani, Phys. Rev. Lett. **54**, 1444 (1985); Phys. Rev. B **50**, 9882 (1994).

[36] K. Hanzawa, J. Phys. Soc. Jpn. **71**, 1481 (2002).

[37] M. Yogi, H. Kotegawa, G. Zheng, Y. Kitaoka, S. Ohsaki,

H. Sugawara, and H. Sato, J. Phys. Soc. Jpn. **74**, 1950 (2005).
[38] N. E. Bickers, D. L. Cox, and J. W. Wilkins, Phys. Rev. Lett. **54**, 230 (1985).
[39] P. J. Brown, in *International Tables for Crystallography*, edited by A. J. C. Wilson, *Mathematical, Physical and Chemical Tables*, Vol. C (Kluwer Academic, Amsterdam, 1999) pp. 450–457.
[40] R. Viennois *et al.*, ISIS Experimental Report (2005).
[41] R. Troć, D. T. Adroja and R. I. Bewley, ISIS Experimental Report (2005).